Mathematical Modelling of Drug Transport and Uptake in a Realistic Model of Solid Tumour

Wenbo Zhan[1], Wladyslaw Gedroyc[2], Xiao Yun Xu[1]

[1]Department of Chemical Engineering, South Kensington Campus,

[2]Department of Radiology, Imperial College Healthcare NHS Trust, St Mary's Hospital,

Imperial College London, UK

Correspondence:

Professor X.Y. Xu

Department of Chemical Engineering

Imperial College London, South Kensington Campus

London SW7 2AZ

Tel: +44 (0) 2075945588

E-mail: yun.xu@imperial.ac.uk

Abstract

Effective delivery of therapeutic agents to tumour cells is essential to the success of most cancer treatment therapies except for surgery. The transport of drug in solid tumours involves multiple biophysical and biochemical processes which are strongly dependent on the physicochemical properties of the drug and biological properties of the tumour. Owing to the complexities involved, mathematical models are playing an increasingly important role in identifying the factors leading to inadequate drug delivery to tumours. In this study, a computational model is developed which incorporates real tumour geometry reconstructed from magnetic resonance images, drug transport through the tumour vasculature and interstitium, as well as drug uptake by tumour cells. The effectiveness of anticancer therapy is evaluated based on the percentage of survival tumour cells by directly solving the pharmacodynamics equation using predicted intracellular drug concentrations. Computational simulations are performed for the delivery of doxorubicin through different administration modes and doses. Our predictions show that continuous infusion is far more effective than bolus injection in maintaining high levels of intracellular drug concentration, thereby increasing drug uptake by tumour cells. On the other hand, bolus injection leads to higher extracellular concentration in both tumour and normal tissues compared to continuous infusion, which is undesirable as high drug concentration in normal tissues may increase the risk of associated side effects.

Keywords: Anticancer therapy, Computational model, Drug transport, MR image-based model, Prostate tumour

Introduction

Cancer is one of the leading causes of death in both developed and developing countries. Currently, cancer is treated primarily by surgery, radiation therapy and chemotherapy. Novel approaches, including gene therapy and antiangiogenesis therapy, have been developed extensively in the last two decades. Except for surgery, most of these therapies depend on the effective delivery of therapeutic agents to tumour cells.

The delivery of therapeutic agents involves multiple processes. On the one hand, these processes are dependent on the physicochemical properties of the drug, such as diffusivity and drug binding to cellular macromolecules. On the other hand, the biologic properties of a tumour, including tumour vasculature, extracellular matrix components, interstitial fluid pressure, tumour cell density and tissue structure and composition, also serve as determinants in these processes [1]. Unfortunately, vasculature in malignant tumours is highly abnormal and heterogeneous. The structural and functional abnormalities of tumour vasculature and microenvironment create a major barrier for drug delivery and contribute to treatment resistance.

Mathematical models are playing an increasingly important role in identifying the factors leading to inadequate drug delivery to tumours and in developing strategies for improved delivery. Although significant progress has been made over the last decade in mathematical modelling of blood flow in tumour vasculature, angiogenesis, and drug transport in solid tumours [2-6], very few attempts have been made to combine blood flow and drug transport in a realistic solid tumour while also accounting for the effect of drug on tumour cells.

Previous mathematical models of drug delivery mainly focused on drug concentration in the interstitial fluid. Baxter and Jain [7-9] set up a numerical platform to investigate the influences of

various factors on the concentration of antibodies (e.g. IgG, $F_{(ab)}$ and $F_{(ab')2}$) in the interstitial fluid. Goh *et al*. [10] applied a similar approach to a 2D hepatoma model to study doxorubicin concentration in the interstitial fluid. Given that the intracellular drug concentration in tumour cells often does not correlate directly with the extracellular drug concentration in interstitial fluid, numerical models should be extended to allow for prediction of intracellular concentration. El-Kareh [11] and Eikenberry [12] used a mathematical model to determine tumour cell uptake of doxorubicin. Although their model incorporated the effect of doxorubicin binding with proteins, it was formulated on a simplified tumour cord geometry, without accounting for the influence of blood and lymphatic vessels or realistic tumour geometry. Detailed analysis of the effectiveness of different drug delivery modes is also lacking. The area under the curve for extracellular drug concentration (AUC_e) was originally used to predict tumour cell kill [13,14]. However, El-Kareh and Secomb [15] noted that not all the data in the literature supported the model based on AUC_e alone, and suggested that exposure time should also be included.

In the present study, an improved mathematical model is applied to a real tumour geometry reconstructed from magnetic resonance images (MRI). The model incorporates the key physical and biochemical processes involved, including time-dependent plasma clearance, drug transport through the blood and lymphatic vessels, extracellular drug transport (convection and diffusion), drug binding with proteins, lymphatic drainage, interactions with the surrounding normal tissue and drug uptake by tumour cells. Anticancer efficacy is evaluated based on the percentage of survival tumour cells by directly solving the pharmacodynamics equation using the predicted intracellular drug concentration. Comparisons are made between different modes of drug administration and doses in a clinically relevant range.

Methods

The mathematical model involves several assumptions. First of all, blood vessels in the tumour are not modelled explicitly; instead, their presence is accounted for by a source term assuming a spatially uniform distribution. It is also assumed that the simulation window is much shorter than the time scale for tumour growth, so that all the tissue and drug related properties are independent of time. Owing to the lack of data on spatial heterogeneity of transport properties, the tumour is treated as a spatially homogeneous region with uniform biological and physical properties [9,10]. The mathematical equations adopted for the coupled interstitial fluid flow and drug transport problem are described below.

Interstitial fluid flow

The mass conservation equation for an incompressible fluid is given by

$$\nabla \cdot \boldsymbol{v} = \left(F_v - F_l\right) \tag{1}$$

where $\boldsymbol{v}$ is the velocity of the interstitial fluid. F_v is the interstitial fluid loss from the blood vessels per unit volume of tumour tissue, and F_l is the fluid absorption rate by the lymphatic system per unit volume of tissue. F_v and F_l are determined by Starling's law

$$F_v = K_v \frac{S}{V}\left[p_v - p_i - \sigma_T\left(\pi_v - \pi_i\right)\right] \tag{2}$$

where K_v is the hydraulic conductivity of the microvascular wall, S/V is the surface area of blood vessels per unit volume of tissue, p_v and p_i are the vascular and interstitial fluid pressure respectively, σ_T represents the average osmotic reflection coefficient for plasma protein, π_v is the osmotic pressure of the plasma, and π_i is that of the interstitial fluid.

The lymphatic drainage, F_l, is related to the pressure difference between the interstitial fluid and lymphatic vessels.

$$F_l = K_l \frac{S_l}{V}\left(p_i - p_l\right) \tag{3}$$

where K_l is the hydraulic conductivity of the lymphatic wall, S_l/V is the surface area of lymphatic vessels per unit volume of tissue, and p_l is the intra-lymphatic pressure.

Since the inter-capillary distance is usually 2-3 orders of magnitude smaller than the length scale for drug transport [9, 10, 26], it is reasonable to treat the tumour and its surrounding tissues as porous media. By ignoring the gravitational effect, the momentum equation is expressed as

$$\frac{\partial(\rho \boldsymbol{v})}{\partial t} + \nabla \cdot (\rho \boldsymbol{v}\boldsymbol{v}) = -\nabla p_i + \nabla \cdot \boldsymbol{\tau} + \boldsymbol{F} \tag{4}$$

where $\boldsymbol{\tau}$ is the stress tensor which is given by

$$\boldsymbol{\tau} = \mu[\nabla \boldsymbol{v} + (\nabla \boldsymbol{v})^T] - \frac{2}{3}\mu(\nabla \cdot \boldsymbol{v})\boldsymbol{I} \tag{5}$$

The last term in equation (4), $\boldsymbol{F}$, represents the Darcian resistance to fluid flow through a porous medium and can be expressed as

$$\boldsymbol{F} = W\mu\boldsymbol{v} + \frac{1}{2} I\rho|\boldsymbol{v}|\boldsymbol{v} \tag{6}$$

where W is a diagonal matrix with all diagonal elements evaluated by:

$$W = \kappa^{-1} \tag{7}$$

Here μ is the dynamic viscosity of the interstitial fluid, $\boldsymbol{I}$ is the prescribed matrix of the inertial loss term, and κ is the permeability of the interstitial space. Since interstitial fluid velocity is very low ($|\boldsymbol{v}|<<1$) [7,16], the inertial loss term can be neglected when compared to the Darcian resistance. In addition, the interstitial fluid is considered as incompressible and Newtonian. Hence, equation (6) can be reduced to

$$\boldsymbol{F} = W\mu\boldsymbol{v} \tag{8}$$

Drug transport

The transport of drug is described by several equations, including those for the free and bound drug in the interstitial fluid and the intracellular drug. In what follows, subscripts *f*, *b* and *i* are used to denote free, bound and intracellular doxorubicin concentrations, respectively.

Free doxorubicin in the interstitial fluid is governed by

$$\frac{\partial C_f}{\partial t} + \nabla \cdot \left(C_f v\right) = D_f \nabla^2 C_f + S_i \tag{9}$$

where C_f is the free doxorubicin concentration and D_f is the corresponding diffusion coefficient. The source term, S_i is the net rate of doxorubicin gained from the surrounding environment, which is given by

$$S_i = S_v + S_b + S_u \tag{10}$$

S_v, S_b and S_u represent the net doxorubicin gained from the blood/lymphatic vessels, association /dissociation with bound doxorubicin-protein and influx/efflux from tumour cells, respectively. These terms are evaluated using the equations described below.

$$S_v = F_s - F_{ls} \tag{11}$$

where F_s is the doxorubicin gained from the blood capillaries in tumour and normal tissues, and F_{ls} is the doxorubicin loss to the lymphatic vessels per unit volume of tissue. Using the pore model [7-9,17] for trans-capillary exchange, F_s and F_{ls} can be expressed as

$$F_s = F_v(1-\sigma)C_v + P\frac{S}{V}(C_v - C_f)\frac{Pe_v}{e^{Pe_v}-1} \tag{12}$$

$$F_{ls} = F_l C_f \tag{13}$$

where C_v is the concentration of doxorubicin in blood plasma, and $\mathrm{Pe_v}$ is the trans-capillary Peclet number defined as

$$\mathrm{Pe_v} = \frac{F_v(1-\sigma)}{P\frac{S}{V}} \tag{14}$$

The net doxorubicin gained due to protein binding and cell uptake is governed by equations (15) and (16), where D_c is the tumour cell density.

$$S_b = k_d C_b - k_a C_f \tag{15}$$

$$S_u = D_c \upsilon - D_c \zeta \tag{16}$$

The bound doxorubicin concentration in the interstitial fluid is described by

$$\frac{\partial C_b}{\partial t} + \nabla \cdot (C_b v) = D_b \nabla^2 C_b + k_a C_f - k_d C_b \tag{17}$$

where C_b is the bound doxorubicin concentration, D_b is the corresponding diffusion coefficient, k_a and k_d are the doxorubicin-protein binding and dissociation rate, respectively.

Because only free doxorubicin can pass through the cell membrane and enter the cell interior [11], the intracellular drug concentration is a function of free doxorubicin concentration in the interstitial fluid.

$$\frac{\partial C_i}{\partial t} = \zeta - \upsilon \tag{18}$$

$$\zeta = V_{max} \frac{C_f}{C_f + k_e \varphi} \tag{19}$$

$$\upsilon = V_{max} \frac{C_i}{C_i + k_i} \tag{20}$$

where C_i is the intracellular doxorubicin concentration, and V_{max} is the rate of trans-membrane transport. The cellular uptake and efflux functions are ζ and υ. k_e and k_i are parameters obtained from experimental data, while φ is the volume fraction of extracellular space.

Tumour geometry

The geometry of a prostate tumour is reconstructed from images acquired from a patient using a 3.0-Tesla MR scanner (DISCOVERY MR750, GE, Schenectady, New York, USA). Multislice anatomical images of the prostate were acquired in three orthogonal planes with echo-planer (EP) sequence, with each image comprising 256 by 256 pixels. Other imaging parameters are given in Table 1.

Table 1. MR imaging parameters

Parameter (unit)	Pixel Size (mm)	Field of View (cm)	Slice Thickness (mm)	Repetition Time (ms)	Echo Time (ms)
	1.250	32.0	7.000	4000	84.4

An example of the MR images is shown in Figure 1 (a) where the tumour region is highlighted in orange, which is surrounded by normal prostatic tissues in pale blue. Transverse images are processed using image analysis software Mimics (Materialise HQ, Leuven, Belgium), and the tumour is segmented from its surrounding normal tissue based on signal intensity values. The resulting smoothed surfaces of the tumour and normal tissues are imported into ANSYS ICEM CFD to generate computational mesh for the entire volume. The dimension of the reconstructed model is approximately 40 mm in length, and the tumour and normal tissue volumes are 2.28×10^{-6} m^3 and 4.42×10^{-5} m^3, respectively. The final mesh consists of 757453 tetrahedral elements which have been tested to produce grid independent solutions.

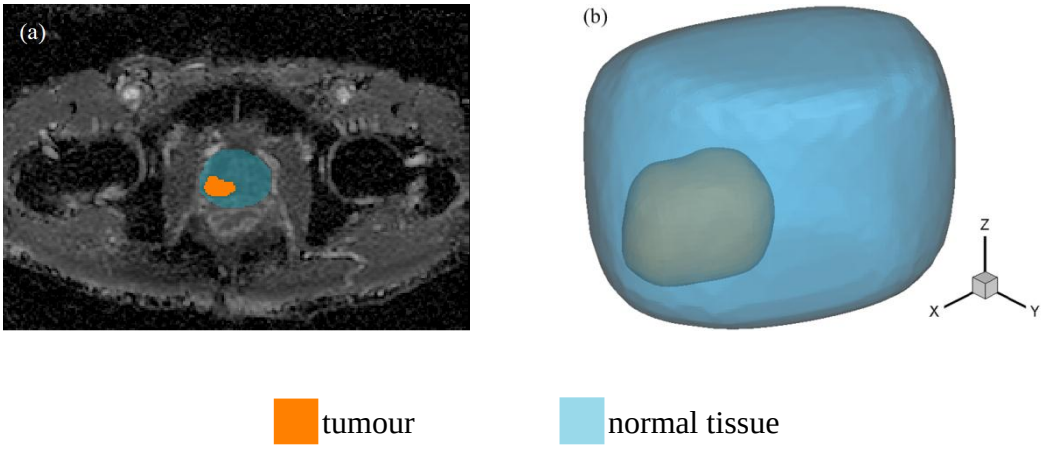

Fig.1. Model geometry: (a) MR image of the prostate tumour and its surrounding tissue; (b) the reconstructed 3-D geometry.

Model parameters

Summarized in Table 2 and Table 3 are model parameters related to the tissue and doxorubicin, respectively. Justifications for the choices of these parameters are given below.

Blood vessel surface area to tissue volume ratio (S/V): The ratio of surface area of blood vessel to tissue volume has a direct influence on the amount of anticancer drug in the interstitial fluid. Its value depends strongly on the type of tissue and stage of tumour growth [18]. Pappenheimer *et al.* measured this in normal tissues [19], while Baxter and Jain [7] recommended using 70 cm^{-1} and 200 cm^{-1} for normal and tumour tissues, respectively.

Tumour cell density (D_c): The volume fraction of extracellular space in a tumour tissue ranges from 0.2 to 0.6 [20]. Assuming an average tumour cell diameter, Eikenberry [12] estimated that tumour cell density ranged from 9.55×10^{15} to 1.53×10^{16} cells/m^3. During chemotherapy treatment, tumour cell density may change as a result of drug uptake, cell proliferation and physiological degradation. This can be described by a pharmacodynamics model [5,21] expressed as

$$\frac{dD_c}{dt} = -\frac{f_{\max} C_i}{EC_{50} + C_i} D_c + k_p D_c - k_a D_c^2 \qquad (21)$$

The first term on the right hand side represents the effect of drug uptake, where f_{max} is the cell-kill rate constant and EC_{50} is the drug concentration producing 50% of f_{max}. k_p and k_a are the cell proliferation rate constant and physiologic degradation rate, respectively. In the present study, cell proliferation and physiologic degradation are ignored.

Diffusion coefficient (D): Diffusion coefficient varies with temperature and is also related to the molecular weight (MW) of the substance [22]. The relationship between diffusion coefficient in water and molecular weight can be represented by [22, 23]

$$D_w = a(MW)^{-b} \tag{22}$$

This equation is used to fit the diffusion coefficients of common anticancer agents in water [24] (Figure 2a). Since doxorubicin has a MW of 544 Da, its diffusion coefficient in water at 37 ^{o}C could be estimated as 3.83×10^{-10} m^2/s. It has also been found that diffusion coefficient in neoplastic tissue deviates from free diffusion in water [20]. For MWs in the range of 376 Da and 66900 Da, the ratio of diffusion coefficient in tumour (D_f) to that in water (D_W) was found to be linearly related to MW

$$D_f / D_w = k\ MW + d \tag{23}$$

Using equation (23), the ratio for doxorubicin is 0.8885 and the diffusion coefficient of doxorubicin in tumour is 3.40×10^{-10} m^2/s (Figure 2b).

At 37 ^{o}C, the relationship between diffusion coefficient (D_f) and MW in normal tissues may be obtained from *in vitro* experimental data [25].

$$D_f = 1.778\times10^{-4}(MW)^{-0.75} \quad (32 < MW < 69000) \tag{24}$$

Based on equation (24), the diffusion coefficient of doxorubicin in normal tissues is calculated as 1.58×10^{-10} m^2/s.

Doxorubicin can bind with high molecular weight proteins (mainly albumin [12]) in the interstitial fluid. In such a case, the diffusion coefficient of the bound component depends mainly

on the protein (i.e. albumin). The effective diffusion coefficient for albumin in VX2 carcinoma was measured as 8.89×10^{-12} m^2/s [12]. Since the bound component has a MW of approximately 69 kDa [10], its diffusion coefficient in normal tissue estimated by equation (24) is 4.17×10^{-12} m^2/s.

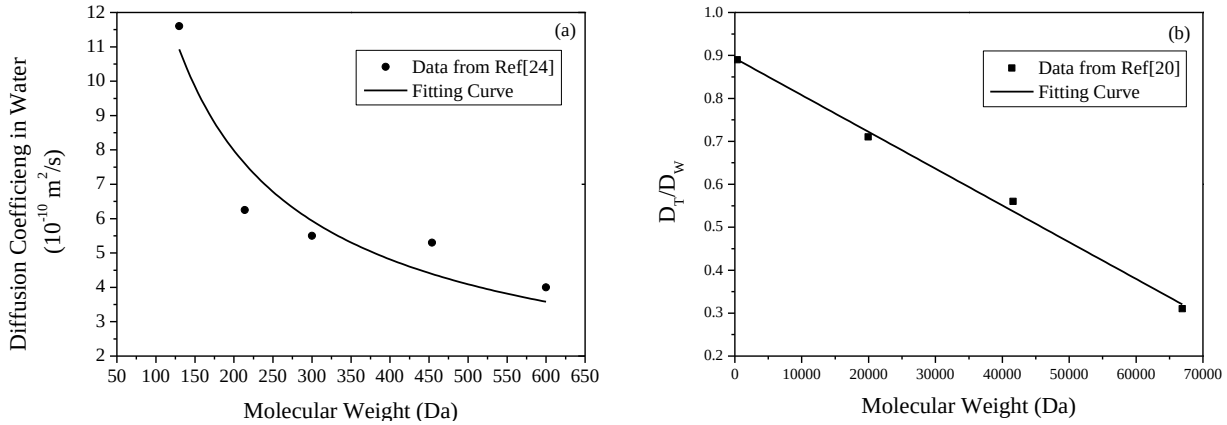

Fig.2. Estimation of doxorubicin diffusion coefficient in tumour tissue. (a) The diffusion coefficient of anticancer drugs in water as a function of molecular weight, using equation (22) [22,23]. For the best fitted curve, a = 380.44, b = 0.73. (b) The relation between diffusion coefficient ratio (tumour to water) and molecular weight. For the best fitted line using equation (23), $k = -8.55948\times10^{-6}$, $d = 0.89317$.

Vascular permeability (P): Vascular permeability coefficient measures the capacity of a blood vessel (often capillary in tumour) wall to allow for the flow of substances in and out of the vasculature. The structure of vessel wall and the molecular size of the transported substance are key determinants of permeability [26]. Estimates of this parameter reported in the literature usually correspond to 'effective permeability', which is on the order of 10^{-7} m/s for albumin in both tumour and normal tissues. For Sulforhodamine B (MW=559 Da), its permeability in normal tissue is 3.4×10^{-7} m/s [27]. Patent is another agent with a similar molecular weight (566

Da) to that of doxorubicin, and its permeability is 3.95×10^{-7} m/s in normal tissue of male frog [28]. Eikenberry [12] assumed the effective permeability of free doxorubicin in tumour to be in the range of 8.1×10^{-7} and 3.7×10^{-6} m/s, whereas Ribba *et al.* [29] used 3.0×10^{-6} m/s in their simulation work. Compared with normal tissues, Gerlowski and Jain [30] found the vessel wall permeability to be 8 times higher in tumour tissues. Using MW for interpolation, Goh [10] assumed the permeability of doxorubicin in tumour tissue to be nearly 8 times higher than in normal tissue. In this study, values of permeability in tumour and normal tissues are assumed to be 3.0×10^{-6} m/s and 3.75×10^{-7} m/s, respectively.

The transmembrane parameters (V_{max}, k_e and k_i) were determined by El-Kareh and Secomb [11] by curve fitting to data obtained from *in vitro* experiments [31]. The pharmacodynamics parameters (f_{max} and EC_{50}) were obtained from experimental results [21].

Drug dose (D_d): The dose of doxorubicin in clinical use is related to the patient's body surface area. In each treatment cycle, the dose is between 50 to 75 mg/m^2 [32]. For a 70 kg patient, dosage of doxorubicin applied in one treatment cycle ranges from 86.5 mg to 129.75 mg.

Plasma pharmacokinetics: Doxorubicin concentration in blood plasma (C_v) is modelled as an exponential decaying function of time. The form of equations depends on the infusion mode.

For continuous infusion, a tri-exponential decay is assumed based on the plasma pharmacokinetics of doxorubicin [11,12].

$$\begin{cases} C_v = \dfrac{D_d}{T}\left[\left(\dfrac{A}{\alpha}\left(1-e^{-\alpha t}\right)+\dfrac{B}{\beta}\left(1-e^{-\beta t}\right)+\dfrac{C}{\gamma}\left(1-e^{-\gamma t}\right)\right)\right] & \left(t<T\right) \\ C_v = \dfrac{D_d}{T}\left[\dfrac{A}{\alpha}\left(e^{\alpha T}-1\right)e^{-\alpha t}+\dfrac{B}{\beta}\left(e^{\beta T}-1\right)e^{-\beta t}+\dfrac{C}{\gamma}\left(e^{\gamma t}-1\right)e^{-\gamma t}\right] & \left(t\geq T\right) \end{cases} \tag{26}$$

where D_d is the dose of doxorubicin and T is the infusion duration. A, B and C are compartment parameters and α, β, γ are compartment clearance rate.

For bolus injection, the terms involving β, γ, B and C represent the compartments with much slower elimination. The drug concentration is assumed to follow an exponential decay based on the plasma pharmacokinetics of doxorubicin [11,12].

$$C_v = D_d A e^{-\alpha t} \tag{27}$$

Table 2. Model parameters for tumour and normal tissues

Parameter	Unit	Tumour Tissue	Normal Tissue	Reference
S/V	m^{-1}	20000	7000	[7-10]
K_v	m/Pa·s	2.10×10^{-11}	2.70×10^{-12}	[7-10]
ρ	kg/m^3	1000	1000	[10]
μ	kg/m·s	0.00078	0.00078	[10]
$1/\kappa$	m^{-2}	4.56×10^{16}	2.21×10^{17}	[7-10]
P_v	Pa	2080	2080	[7-10]
π_v	Pa	2666	2666	[7-10]
π_i	Pa	2000	1333	[7-10]
σ_T		0.82	0.91	[7-10]
$K_l S_l/V$	$(Pa\cdot s)^{-1}$	0	4.17×10^{-7}	[10]
P_l	Pa	0	0	[10]
D_c	$10^5 cell/m^3$	1×10^{10}	1×10^{10}	[11,12]
φ		0.4	-	[11,12]

Table 3. Model parameters for doxorubicin

Parameter	Unit	Free Doxorubicin	Bound Doxorubicin	Reference
P_{Tumour}	m/s	3.00×10^{-6}	-	-
P_{Normal}	m/s	3.75×10^{-7}	-	-
D_{Tumour}	m^2/s	3.40×10^{-10}	8.89×10^{-12}	-
D_{Normal}	m^2/s	1.58×10^{-10}	4.17×10^{-12}	-
MW	kg/mol	0.544	69.0	[10,11]
σ		0.15	-	[10]
k_a	s^{-1}	0.833	-	[11,12]
k_d	s^{-1}	-	0.278	[11,12]
V_{max}	$kg/10^5$cells s	4.67×10^{-15}	-	[11,31]
k_e	kg/m^3	2.19×10^{-4}	-	[11,31]
k_i	kg/m^3	1.37×10^{-12}	-	[11,31]
D_d	kg	$8.56\sim12.84\times10^{-5}$	-	[32]
A	m^{-3}	74.6 (infusion)	74.6 (infusion)	[11,12,33]
		130.0 (bolus)	130.0 (bolus)	[11,12,33]
B	m^{-3}	2.49	2.49	[11,12,33]
C	m^{-3}	0.552	0.552	[11,12,33]
α	s^{-1}	2.69×10^{-3}(infusion)	2.69×10^{-3}(infusion)	[11,12,33]
		2.43×10^{-3}(bolus)	2.43×10^{-3}(bolus)	[11,12,33]
β	s^{-1}	2.83×10^{-4}	2.83×10^{-4}	[11,12,33]
γ	s^{-1}	1.18×10^{-5}	1.18×10^{-5}	[11,12,33]

f_{max}	s^{-1}	1.67×10^{-5}	-	[21]
EC_{50}	$kg/10^5 cells$	5×10^{-13}	-	[21]

Numerical Methods

The mathematical models described above are implemented in ANSYS-Fluent, which is a finite volume based computational fluid dynamics (CFD) code (ANSYS Inc., Canonsburg, USA). The momentum and drug transport equations are discretised using the second order upwind scheme, and the SIMPLEC algorithm is employed for pressure-velocity coupling. The Gauss-Seidel smoothing method is used to update values at nodal points after each iteration step. Convergence is controlled by setting residual tolerances of the momentum equation and the drug transport equations to be 1×10^{-5} and 1×10^{-8}, respectively. In order to generate initial conditions for the transient simulation, the interstitial fluid flow equations are firstly solved to obtain a steady-state solution in the entire computational domain. Following this, the obtained pressure and velocity values are applied at time zero for the simulation of drug transport and cellular uptake. The first order implicit backward Euler scheme is used for temporal discretisation, and a fixed time step size of 10 seconds is chosen. This time step is deemed sufficiently fine based on a time step sensitivity test. The initial doxorubicin concentrations are assumed to be zero.

There are two boundary surfaces in this model: an internal boundary between the tumour tissue and normal tissue, and the outer surface of the normal tissue. At the internal boundary, conditions of continuity of the interstitial pressure and fluid flux are applied. At the outer surface, a constant relative pressure of 0 Pa and zero flux of drug concentration are assumed.

Results

The transport of drug depends strongly on the microenvironment in tumour and normal tissues. The interstitial fluid pressure (IFP) is an important parameter determining the exchange of drug between the interstitial space and vasculature. By solving equations (1) - (8) for a vascular pressure of 2080 Pa [7-10], the flow field can be resolved and the predicted mean IFP are found to be 1500 Pa in tumour and 40 Pa in normal tissue. Experimental studies suggested that the IFP in normal tissue was in the range of -400 Pa to 800 Pa [34, 35], and in tumour 586.67 Pa to 4200 Pa [36].

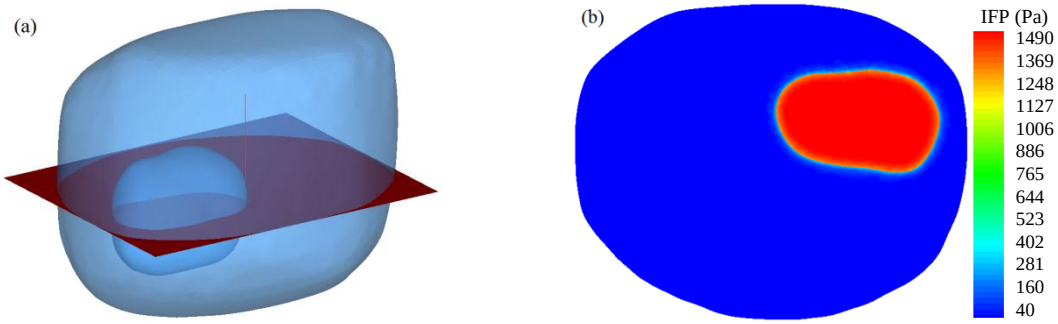

Fig.3. Interstitial fluid pressure in tumour and normal tissues. (a) location of the cross section; (b) interstitial fluid pressure at the defined cross section.

Figure 3 shows the spatial IFP distribution at a transverse plane. It is clear that IFP is much higher in the tumour than its surrounding normal tissue, and there is a large gradient in a thin layer at the interface between the two regions.

Comparison of different drug administration modes

The cytotoxic effect of doxorubicin on tumour cells is evaluated for bolus injection and continuous infusions with different infusion durations. Given that doxorubicin is carried by

blood into the tumour and normal tissues, its concentration in blood should be examined when evaluating its anticancer effectiveness. The predicted time course of doxorubicin blood concentration, for a total dose of 50 mg/m^2 administered by different injection modes, is compared in Figure 4. The dose is chosen within a clinically relevant rang. The results show that with increasing infusion duration, the peak doxorubicin blood concentration decreases. In addition, although fast infusion leads to higher concentrations at the beginning of the treatment, doxorubicin concentration in blood falls much faster after the infusion ends.

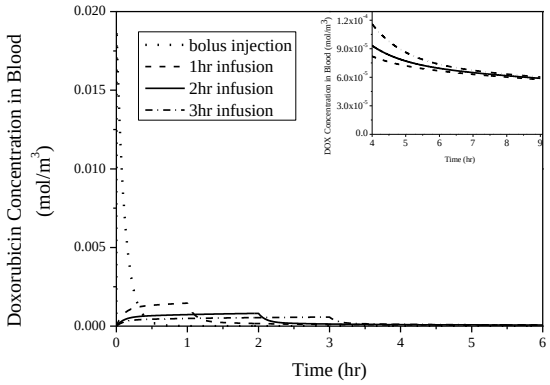

Fig.4 Doxorubicin concentration in plasma as a function of time after start of treatment, for bolus injection and continuous infusion of various indicated durations (dose = 50 mg/m^2).

Free and bound doxorubicin extracellular concentrations in tumour and normal tissues are shown in Figure 5 and Figure 6, respectively. Regardless of the injection mode, both free and bound doxorubicin concentrations increase rapidly during the initial period following drug administration. Doxorubicin concentrations in tumour and normal tissues reach a much higher peak with bolus injection. Although doxorubicin concentration drops to a low level after the infusions ends for all modes of administration, continuous infusions are able to maintain a slightly higher concentration than bolus injection. Comparing doxorubicin extracellular concentrations in Figures 5 and 6 with the blood concentration in Figure 4, the concentration

curves have identical shapes for a given administration mode. This means that blood concentration has a direct influence on the extracellular concentration for both free and bound doxorubicin.

The extracellular concentration of free doxorubicin in tumour is much higher than in normal tissue. The same is true for bound doxorubicin, mainly owing to the difference in permeability. Since permeability in tumour tissue is much higher than in normal tissue, more drugs can permeate through the vessel wall into the interstitial space in tumour. Moreover bound doxorubicin concentrations are approximately 3 times of the free doxorubicin concentrations in tumour, indicating that most doxorubicin in the interstitial fluid is in bound form.

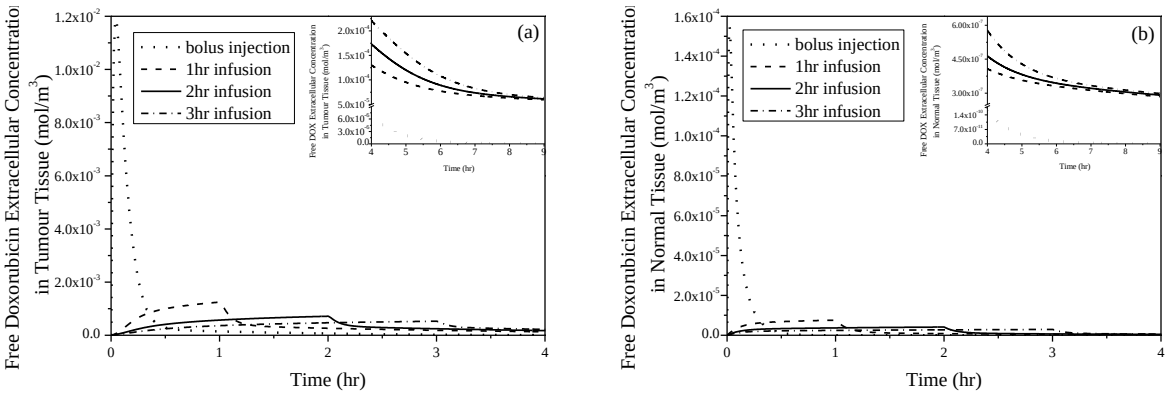

Fig.5. Spatial mean free doxorubicin extracellular concentration as a function of time under bolus injection and different infusion durations. (a) in tumour tissue, (b) in normal tissue (dose = 50 mg/m^2).

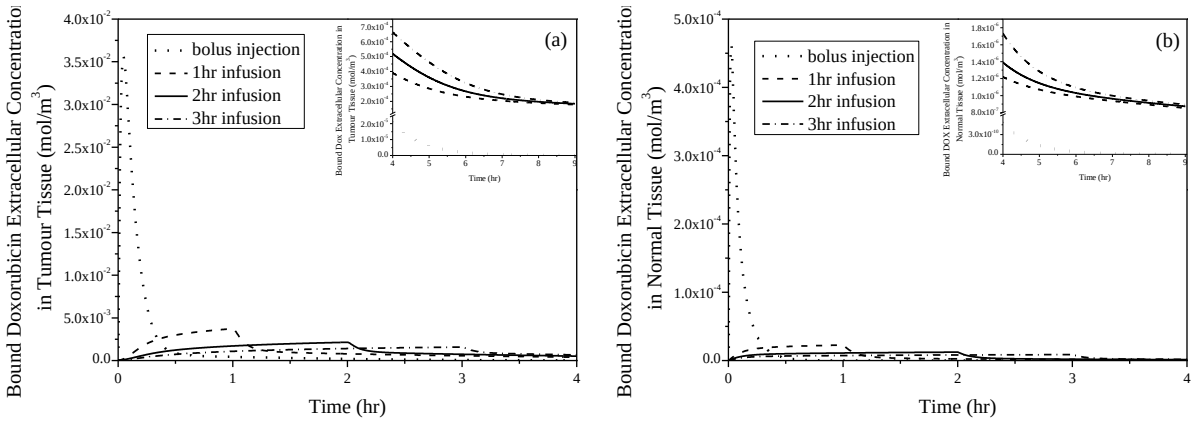

Fig.6. Spatial mean bound doxorubicin extracellular concentration as a function of time under bolus injection and different infusion durations. (a) in tumour tissue, (b) in normal tissue (dose = 50 mg/m^2)

Figure 7 shows the free doxorubicin extracellular concentration at a cross-section (defined in Figure 2) at 0.5 hour under 2-hour continuous infusion. Free doxorubicin extracellular concentration is much higher in tumour than in normal tissue. The distribution is uniform in each region except near the tumour boundary where a large concentration gradient exists. This is desirable as transport of doxorubicin from tumour to normal tissue should be minimised in order to maintain a high level of doxorubicin concentration in tumour.

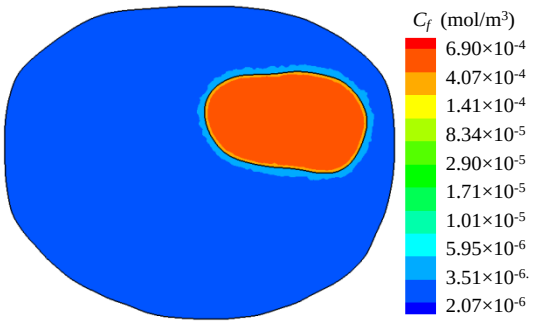

Fig.7. Spatial distribution of extracellular concentration of free doxorubicin in tumour and normal tissues (2-hour infusion, time=0.5 hr).

Figure 8 presents the intracellular doxorubicin concentration in tumour under bolus injection and various continuous infusions. The intracellular concentration displays a sharp rise at the beginning until it reaches a peak, and then decreases. During the initial phase, the rate of increase in doxorubicin concentration slows down with increasing infusion duration. Compared to bolus injection, continuous infusions lead to a slower reduction in intracellular concentration which also remains at a much higher level after infusion ends.

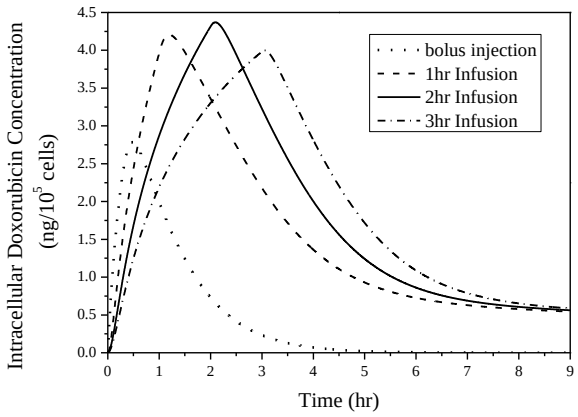

Fig.8. Doxorubicin intracellular concentration as a function of time, for bolus injection and continuous infusions of various durations (dose = 50 mg/m^2).

For continuous infusions, longer infusion durations tend to slow down the increase in intracellular concentration at the initial phase of treatment, but produce a higher peak until an optimal duration of infusion is reached. Here, the highest intracellular concentration is found for a 2-hour continuous infusion. Moreover, for continuous infusion with different durations, intracellular concentrations reach a very similar level after the infusions end.

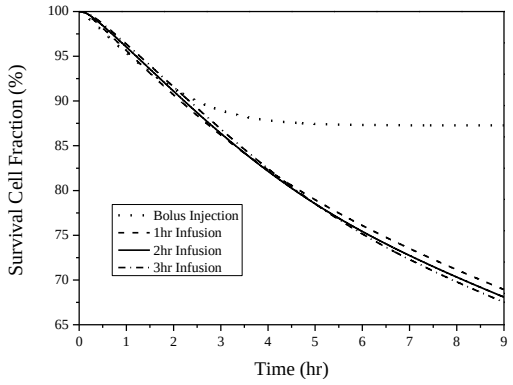

Fig.9. Predicated percentage tumour cell survival under bolus injection and continuous infusions of various durations (dose = 50 mg/m^2).

Figure 9 shows the percentage of tumour cell survival by applying the pharmacodynamics model described by equation (21). To focus on the effect of drug on cell kill, tumour cell proliferation and physiological degradation are ignored. As can be observed, the cytotoxic effect of bolus injection on tumour cells is significantly lower than that of continuous infusions. However, the effect of infusion duration seems to be insignificant for the limited range of infusion durations examined, with a difference of up to 2% between the slower (3 hours) and faster infusion (1 hour).

On the other hand, bolus injection causes higher extracellular concentration in normal tissues than continuous infusions, which is undesirable as high drug concentration in normal tissue may increase the risk of side effects in patients.

Effect of dose level

Another controllable parameter in chemotherapy is the dose level of anticancer drugs. In current clinical use, doxorubicin dose ranges from 50 mg/m^2 to 75 mg/m^2, hence the effect of dose on drug effectiveness is examined within this range.

Comparison is made between different doses (50, 60 and 75mg/m^2) for a 2-hour continuous infusion, as shown in Figure 10. With increasing doses, doxorubicin concentrations in all regions increase in proportion to the dose level, since a high dose increases the amount of drug delivered to both the tumour and normal tissues.

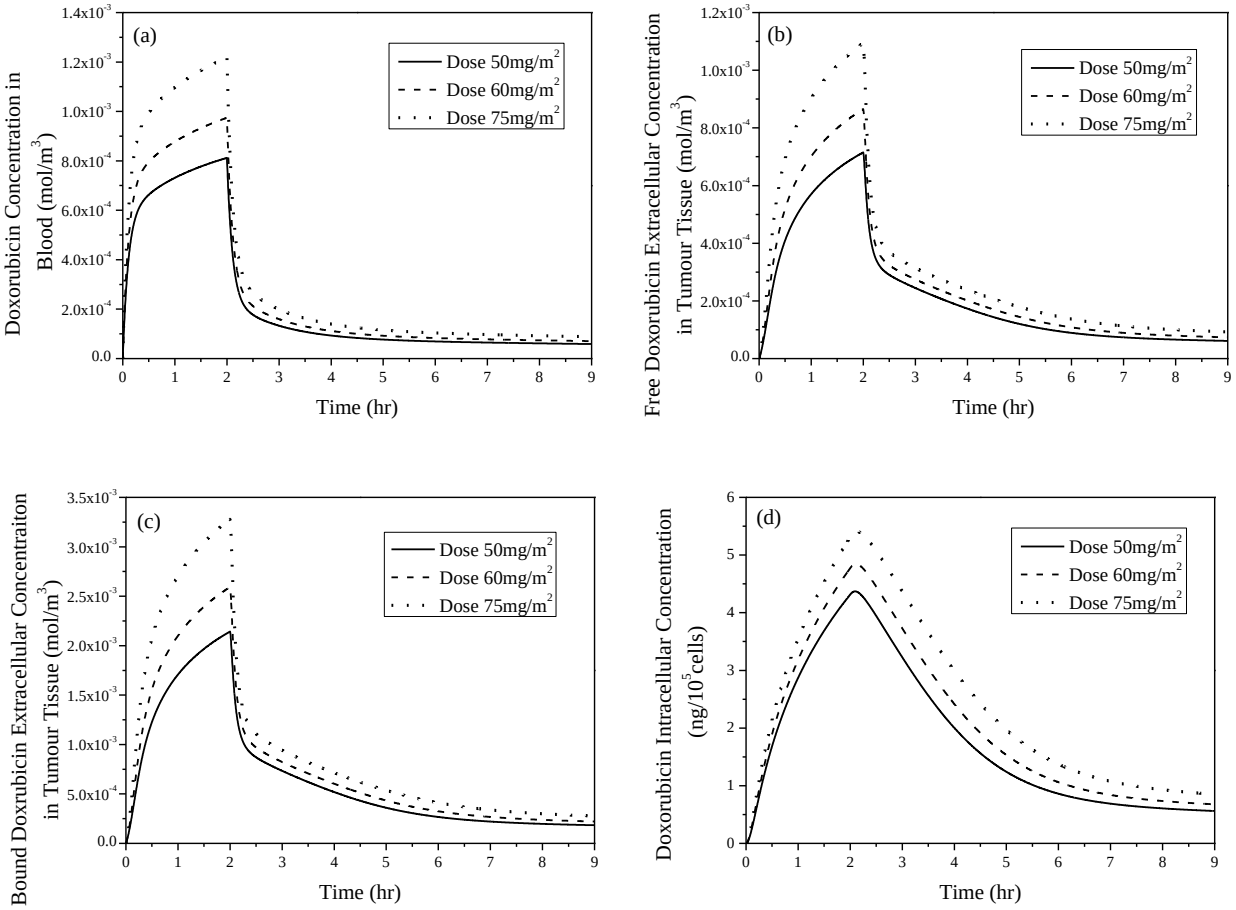

Fig.10 Spatial mean doxorubicin concentration as a function of time under 2-hour infusion duration (for a 70kg patient).(a) doxorubicin blood concentration, (b) free doxorubicin extracellular concentration, (c) bound doxorubicin extracellular concentration, (d) intracellular concentration.

The percentage of tumour cell survival is compared in Figure 11. The results show that the cytotoxic effect of doxorubicin on tumour cells increases with the dose level, with the difference between low (50 mg/m^2) and high doses (75 mg/m^2) being 2.5 %.

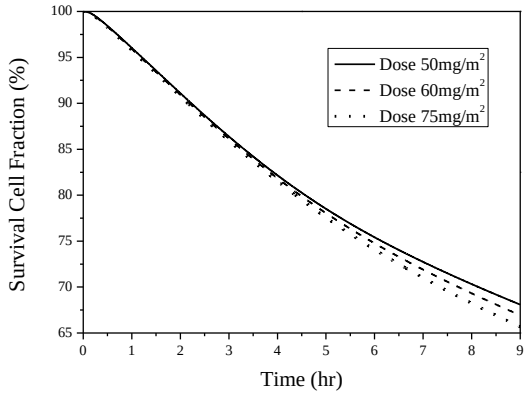

Fig.11 Predicated percentage of tumour cell survival under various doses.

Discussion

After intravenous infusion, anticancer drugs need to experience the following steps before reaching the interior of tumour cells: clearance from plasma, passing through the microvascular wall, diffusion and convection in extracellular space and crossing the cell membrane. The time scale for each transport step is different owing to the different properties of microvasculature, interstitial fluid and the kinetics of cellular uptake. Data in the literature suggest that there is a delay between intracellular and extracellular drug concentration levels [11]. This is the reason why extracellular concentrations need to maintain at a high level for long enough for cellular uptake. Our simulation results show that the peak intravascular doxorubicin concentration is achieved approximately 5.67 min later than the corresponding peak extracellular concentration. Comparisons between bolus injection and continuous infusions suggest that the latter are more

effective in maintaining high levels of extracellular doxorubicin over longer time (see Figure 5), thereby raising intravascular levels (Figure 8) and enhancing cellular uptake.

With regard to the effect of infusion duration, although the predicted difference in percentage cell survival is insignificant between the 3-hour and 1-hour infusion, longer infusion duration is beneficial for sustained extracellular and intracellular levels over time. An interesting finding is that the maximum intracellular doxorubicin concentration is achieved with the 2-hour continuous infusion.

Anticancer effectiveness is usually evaluated by cell survival fraction, which can be predicted by different mathematic models. As an improvement of the AUC model [14], the peak intracellular concentration model [11,12] agrees better with experimental data. However, this model predicts the best cell kill fraction for the entire treatment only, without giving any information on how cell survival changes with time. Knowledge of temporal variation of cell survival is important since both extra- and intracellular drug concentrations change with time during a treatment period. The pharmacodynamics model employed in this study overcomes this shortcoming by providing temporal profiles of cell survival fraction. In addition, the model allows cell proliferation and degradation to be included, making it a step closer to mimicking an *in vivo* environment. Although the effects of cell proliferation and degradation are neglected in the present study, results shown in Figures 9 and 11 demonstrate that sustained levels of extracellular concentration lead to higher intracellular concentration over time, which can cause more serious tumour cell killing.

The present study involves several assumptions. Firstly, tumour cell proliferation and physiological degradation are ignored in order to isolate the effect of drug on tumour cell kill. In

reality, tumour cells may proliferate and die, which would have a direct influence on tumour cell density, and indirectly affect the extra- and intracellular concentrations [21]. However, because the time scale of tumour cell proliferation is typically much larger than the simulation time which corresponds to one treatment of a few hours only [10], the effect of this assumption is considered to be minor. For longer simulation time, cell proliferation and degradation should be incorporated by solving equation (21) with non-zero values for k_p and k_a. Secondly, the properties of tumour and normal tissues are assumed to be constant. These may vary with the tissue type, growth stage and individual conditions of a patient [7, 8]. Moreover, transport properties and vascular distribution are likely to be heterogeneous and non-uniform in a given tumour. All these properties will affect the way anticancer drugs are transported to tumour cells, and eventually the effectiveness of an anticancer treatment. The effect of this assumption can be evaluated by carrying out a sensitivity study with different vascular densities. The model parameters adopted in this study correspond to average and representative values for tumour and normal tissues extracted from the literature, which are sufficient for qualitative study. For more detailed quantitative analysis, tumour-specific and patient-specific information would be required. While numerical models can be used to predict qualitative trend and identify opportunities for optimal treatments, experimental studies are needed to provide the essential input data and for model validation.

Conclusion

In conclusion, this numerical study shows that bolus injection is much less effective in tumour cell kill than continuous infusion, the latter being not only effective in improving the cytotoxic effect of doxorubicin on tumour cells, but also in reducing doxorubicin level in normal tissue. Our computational results also show that rapid continuous infusion leads to faster cell kill at the

beginning of the treatment, but slow infusion modes perform better over time. For a given dose, there may exist an optimal infusion duration for maximum anticancer effectiveness without increasing drug concentration in normal tissues.

Increasing drug dose can increase concentration levels in all regions of tumour, and improve the effectiveness of anticancer treatment. Whist consideration must be given to potential side effect, which limits the dosage that can be used in practice, the highest tolerable dose gives best results.

Reference

[1] Jang, S.H.; Wientjes, M.G.; Lu, D; Au, J.L. Drug delivery and transport to solid tumors. *Pharm. Res*., **2003**, *20*, 1337-1350.

[2] McDougall, S.R.; Anderson, A.R.A., Chaplain, M.A.J.; Sherratt, J. A. Mathematical modelling of flow through vascular networks: Implications for tumour-induced angiogenesis and chemotherapy strategies. *Bull. Math. Biol.*, **2002**, *64*, 673-702.

[3] Pozrikidis, C.; Farrow, D.A.A model of fluid flow in solid tumours. *Ann. Biomed. Eng*., **2003**, *31*, 181-194.

[4] Wijeratne, N.S.; Hoo, K.A. Understanding the role of the tumour vasculature in the transport of drugs to solid cancer tumours. *Cell Prolif*., **2007**, *40*, 283-301.

[5] Liu C., Krishnan J., Xu X.Y. A systems-based mathematical modelling framework for investigating the effect of drugs on solid tumours, *Theor. Biol. Med. Model*, **2011**, *8*, 45-65.

[6] Zhao J.B.; Salmon H.; Sarntinoranont M. Effect of heterogeneous vasculature on interstitial transport within a solid tumor. *Microvas. Res.*, **2007**, *73*, 224-236.

[7] Baxter L.T.; Jain R.K. Transport of fluid and macromolecules in tumours. I role of interstitial pressure and convection. *Microvas. Res*., **1989**, *37*, 77–104.

[8] Baxter L.T., Jain R.K. Transport of fluid and macromolecules in tumours. II role of heterogeneous perfusion and lymphatics. *Microvas. Res*., **1990**, *40*, 246-263.

[9] Baxter L.T., Jain R.K. Transport of fluid and macromolecules in tumours. III role of binding and metabolism. *Microvas. Res*., **1991**, *41*, 5-23.

[10] Goh Y.M.; Kong H.L.; Wang C.H. Simulation of the Delivery of Doxorubicin to Hepatoma. *Pharm. Res.*, **2001**, *18*, 761-770.

[11] El-Kareh A.W.; Secomb T.W. A mathematical model for Comparison of bolus injection, continuous infusion, and liposomal delivery of doxorubicin to tumour cells. *Neoplasia*, **2000**, *2*, 325-388.

[12] Eikenberry S. A tumor cord model for Doxorubicin delivery and dose optimization in solid tumors. *Theoretical Biology and Medical Modelling*, **2009**, *6*, 16-36.

[13] Greene R.F.; Collins J.M.; Jenkins J.F.; Speyer J.L.; Myers C.E. Plasma pharmacokinetics of adriamycin and adriamycinol: implications for the design of in vitro experiments and treatment protocols. *Cancer Research,* **1983,** *43*, 3417-3421.

[14] Ozawa S.; Sugiyama Y.; Mitsuhashi Y.; Kobayashi T.; Inaba M. Cell killing action of cell cycle phase-specific antitumour agents is dependent on concentration-time product. *Cancer Chemother Pharmacol*, **1998**, *21*, 185-190.

[15] El-Kareh A.W.; Secomb T.W. Two-mechanism peak concentration model for cellular pharmacodynamics of doxorubicin. *Neoplasia,* **2005**, *7*, 705-713.

[16] Butler T.P.; Grantham F.H.; Gullino P.M. Bulk transfer of fluid in the interstitial compartment of mammary tumors. *Cancer Research*, **1975**, *35*, 3084-3088.

[17] Deen W.M. Hindered transport of large molecules in liquid-filled pores. *AIChE Journal*, **1987**, *33*, 1409-1425.

[18] Hilmas D.E.; Edward L.; Gillette D.Y.M. Morphometric analyses of the microvasculature of tumors during growth and after x-irradiation. *Cancer*, **1974**, *33*, 103–110.

[19] Pappenheimer J.R.; Renkin E.M.; Borrero L.M. Filtration, diffusion and molecular sieving through peripheral capillary membranes: A contribution to the pore theory of capillary permeability. *Amer. J Physiol*, **1951**, *82*, 13-46

[20] Nugent L.J.; Jain R.K. Extravascular Diffusion in Normal and Neoplastic Tissues. *Cancer Research*, **1984,** *44*, 238-244.

[21] Eliaz R.E.; Nir S.; Marty C.; Szoka F.C, Jr. Determination and Modeling of Kinetics of Cancer Cell Killing by Doxorubicin and Doxorubicin Encapsulated in Targeted Liposomes. *Cancer Research*, **2004**, *64*, 711-718.

[22] Jain R.K. Transport of Molecules in the Tumor Interstitium: A Review, Extravascular Diffusion in Normal and Neoplastic Tissues. *Cancer Research*, **1987**, *47*, 3039-3051.

[23] Granath, K.A.; Kvist, B.E. Molecular weight distribution analysis by gel chromatography on Sephadex. *J Chromatogr*. **1967**, *28*, 69-81.

[24] Saltzman W.M.; Radomsky M.L. Drugs released from polymers: diffusion and elimination in brain tissue. *Chemical Engineering Science*, **1991**, *46*, 2429-2444.

[25] Swabb E.A.; James W, Gullino P.M. Diffusion and convection in normal and neoplastic tissues. *Cancer Research*, **1974**, *34*, 2814-2822.

[26] Yuan F.; Dellian M.; Fukumura D.; Leunig M.; Berk D.A.; Torchilin V.P.; Jain R.K. Vascular permeability in a human tumor xenograft: molecular size dependence and cutoff size. *Cancer Research*, **1995**, *55*, 3752-3756.

[27] Wu N.Z.; Klitzman B., Rosner G., Needham D., Dewhirst M.W. Measurement of Material Extravasation in Microvascular Networks Using Fluorescence Video-Microscopy. *Microvasc Res*, **1993**, *46*, 231-253.

[28] Curry F.E.; Huxley V.H.; Adamson R.H. Permeability of single capillaries to intermediate-sized colored solutes. *Am J Physiol*., **1983**, *245*, 495-505.

[29] Ribba B.; Marron K.; Agur Z.; Alarcón T.; Maini P.K. A mathematical model of Doxorubicin treatment efficacy for non-Hodgkin's lymphoma: investigation of the current protocol through theoretical modelling results. *Bull Math Biol*, **2005**, *67*, 79-99.

[30] Gerlowski L.E.; Jain R.K. Microvascular permeability of normal and neoplastic tissues. *Microvasc Res*, **1986**, *31*, 288-305.

[31] Kerr D.J.; Kerr A.M.; Freshney R.I.; Kaye S.B. Comparative intracellular uptake of adriamycin and 4'-deoxydoxorubicin by nonsmall cell lung tumor cells in culture and its relationship to cell survival. *Biochem Pharmacol*, **1986**, *35*, 2817-2823.

[32] Brunton L.; Lazo J.; Parker K. *Goodman & Gilman's the pharmacological basis of therapeutics*. McGraw-Hill: New York, **2005**.

[33] Robert J.; Illiadis A.; Hoerni B.; Cano J.P.; Durand M.; Lagarde C. Pharmacokinetics of adriamycin in patients with breast cancer: correlation between pharmacokinetic parameters and clinical short-term response. *Eur J Cancer Clin Oncol*, **1982**, *18*, 739-45.

[34] Raghunathan S.; Evans D.; Sparks J.L. Poroviscoelastic modelling of liver biomechanical response in unconfined compression. *Annals of Biomedical Engineering*, **2010**, *38*, 1789-1800.

[35] Guyton A.C.; Hall J.E. *Textbook of medical physiology*, 11th ed.; Elsevier Saunders: Philadelphia, **2006**.

[36] Boucher Y.; Jain R.K. Microvascular pressure is the principal driving force for interstitial hypertension in solid tumors: implications for vascular collapse. *Cancer Research*, **1992**, *52,* 5110-5114.